Title: Toxicokinetic modeling of folpet fungicide and its ring-biomarkers of exposure in humans.

Authors: Heredia-Ortiz R, Berthet A, Bouchard M

Journal: Journal of Applied Toxicology

Year: 2013

Issue: 33

Volume: 7

Pages: 607-617

DOI: 10.1002/jat.1782

Toxicokinetic modeling of folpet fungicide and its ring-biomarkers of exposure in humans

Roberto Heredia-Ortiz[a], Aurélie Berthet[a,b], Michèle Bouchard[a,*]

[a] Département de santé environnementale et santé au travail, Chaire d'analyse et de gestion des risques toxicologiques and Institut de recherche en santé publique de l'Université de Montréal (IRSPUM), Faculté de Médecine, Université de Montréal, C.P. 6128, Succursale Centre-ville, Montréal, Québec, Canada, H3C 3J7

[b] Institute for Work and Health, Rue du Bugnon 21, 1011 Lausanne, Switzerland

*Correspondence to:

M. Bouchard, Département de Santé environnementale et santé au travail, Université de Montréal, C.P. 6128, Succursale Centre-ville, Montréal, Québec, H3C 3J7, Canada.
E-mail: michele.bouchard@umontreal.ca
Telephone number: (514) 343-6111 ext 1640
Fax number: (514) 343-2200

Short title: Toxicokinetic modeling of folpet biomarkers in humans

ABSTRACT

A human in-vivo toxicokinetic model was built to allow a better understanding of the toxicokinetics of folpet fungicide and its key ring biomarkers of exposure: phthalimide (PI), phthalamic acid (PAA) and phthalic acid (PA). Both PI and the sum of ring-metabolites, expressed as PA equivalents (PA_{eq}), may be used as biomarkers of exposure. The conceptual representation of the model was based on the analysis of the time course of these biomarkers in volunteers orally and dermally exposed to folpet. In the model, compartments were also used to represent the body burden of folpet and experimentally relevant PI, PAA and PA ring metabolites in blood and in key tissues as well as in excreta, hence urinary and faeces. The time evolution of these biomarkers in each compartment of the model was then mathematically described by a system of coupled differential equations. The mathematical parameters of the model were then determined from best-fits to the time courses of PI and PA_{eq} in blood and urine of five volunteers administered orally 1 mg/kg and dermally 10 mg/kg of folpet. In the case of oral administration, the mean elimination half-life of PI from blood (either through faeces, urine or metabolism) was found to be 39.9 h as compared to 28.0 h for PA_{eq}. In the case of a dermal application, mean elimination half-life of PI and PA_{eq} was estimated to be 34.3 and 29.3 h, respectively. The average final fractions of administered dose recovered in urine as PI over the 0-96 h period were 0.030% and 0.002%, for oral and dermal exposure, respectively. Corresponding values for PA_{eq} were 24.5% and 1.83%, respectively. Finally, the average clearance rate of PI from blood calculated from the oral and dermal data was 0.09 ± 0.03 mL/h and 0.13 ± 0.05 mL/h while the volume of distribution was 4.30 ± 1.12 L and 6.05 ± 2.22 L, respectively. It was not possible to obtain the corresponding values from PA_{eq} data due to the lack of blood time course data.

Keywords: Folpet, Toxicokinetics, Biomarkers.

Table of Contents – Short abstract

A human in-vivo toxicokinetic model was built to allow a better understanding of the toxicokinetics of folpet fungicide and its key biomarkers of exposure, and to simulate the transformation of folpet into PI and other ring-metabolites: phthalamic (PAA) and phthalic acids (PA). The model closely reproduced the time courses of PI in blood and urine as well as total ring-metabolites in urine of five volunteers administered orally 1 mg/kg and dermally 10 mg/kg of folpet.

INTRODUCTION

Folpet (CAS 133-07-3) is a fungicide commonly used in agricultural environments. It is applied for preventive treatment of plants to control mildew, gray mold, spoilage fungi and wood rot fungi. Folpet is a broad-spectrum contact protectant fungicide which denatures fungal proteins by reacting with their thiol groups (USEPA, 1999; Gordon, 2010). In humans, it is classified as probable human carcinogen (B2) by the US Environmental Protection Agency (1975, 1999) based on an increased incidence of duodenum tumors in mice chronically exposed to high doses by gavage. It is also considered as a severe irritant of the eyes, skin, nose and throat (Lisi *et al.*,1987; Guo *et al.*,1996; Gordon, 2010).

Although folpet is widely used in agriculture, there is a paucity of data to assess the importance of exposure to this compound in workers (Zainal and Que, Hee 2003; Lebailly *et al*., 2006) and no biomonitoring data is available in literature to our knowledge. Moreover, the human toxicokinetics of folpet and its ring metabolites is not fully understood, although its knowledge is necessary to interpret biomonitoring data in field studies.

The majority of toxicokinetic data on folpet was obtained from *in vivo* experiments in animals following radiolabelled-dosing as well as *in vitro* studies. These studies allowed the identification of the main metabolic pathway of folpet (Fig. 1). According to these studies, folpet is rapidly split at the N-S link when it is in contact with thiol groups and the reaction is enhanced in acid conditions (Gordon *et al*., 2001; Gordon, 2010). From this non-enzymatic process, the ring-metabolite PI and a thiocarbonyl chloride are formed. The initial ring-metabolite of folpet, PI, is rapidly hydrolyzed to phthalamic acid (PAA) mainly and in turn to phthalic acid (PA), according to animal studies (Gordon *et al*., 2001; Zainal and Que Hee, 2003; Canal-Raffin *et al*., 2008; Gordon, 2010).

Following oral or intraperitonal administration of ring-labelled folpet, between 90 and 100% of dose were excreted in the urine of rats over a 24-h period post-dosing. This is based on the study of Wood *et al*. (1991) showing that 92% of an orally administered dose of 10 mg/kg of ^{14}C-labelled folpet in rats were recovered in urine as ^{14}C equivalents as compared to 6% in faeces. Couch *et al.* (1977) also indicated that virtually 100% of an intraperitoneal dose of 6 mg/kg of 14C-folpet were recovered in urine as ^{14}C equivalents and 1.7% in faeces over the 24-h period post-dosing.

When PI metabolite was orally administered to rats, about 80% of the administered dose were metabolized and excreted in urine as PAA, 7% were found as PA, and less than 1% of the dose was recovered as PI in urine (Chasseaud *et al*., 1974). PAA also represented the main metabolite (*i.e.* 80%) when labeled ^{14}C-folpet was orally administered to rats (Chasseaud, 1980). However, they reported that this metabolite was unstable in urine. The rat studies of Chasseaud *et al*. (1974, 1980) thus showed that PAA and PA appear as quantitatively more important biomarkers than PI. Nonetheless, PA is not a metabolite

specific to folpet; it is also a derivative of phthalates, which are ubiquitous molecules in our environment (Blount *et al*., 2000; Silva *et al*., 2007).

Furthermore, in the only dermal penetration study on folpet in animals, Shah *et al*. (1987) estimated a low dermal absorption fraction, as assessed from analysis of radioactivity in skin and carcasses at 72 h post-application of a low, medium and high dose of ^{14}C-trichloromethyl labelled folpet in Fisher 344 rats as well as in urine and faeces collected over the 72-h period post-dosing. On average, 12% of the low dose of folpet were calculated to be absorbed through the skin during that time (application of 0.1 µmol/cm^2 on 2.8 and 5.6 cm^2 of young and adult rats, respectively) as compared to only 3 and 1% for the two higher doses (application of 0.5 and 2.7 µmol/cm^2, respectively).

With regard to elimination kinetics of PI, Canal-Raffin *et al*. (2008) reported an elimination half-life of on average 2.5 h in plasma following a single intraperitoneal folpet dose of 10 mg/kg in Wistar rats. Ackermann *et al*. (1978) also estimated a PI half-life of 2 h in rat fetuses following an oral administration of 2.5 mg/kg of ^{15}N-phthalimide to pregnant Wistar-strain albino rats and observed a fast metabolism of PI into PAA. This latter metabolite is then transformed to PA, the final ring-metabolite of folpet (Williams and Blanchfield, 1974). On the other hand, in an *in vitro* study, Gordon *et al*. (2001) reported a half-life of labelled-folpet added to human blood of 4.9 seconds.

Recently, the human time courses of PI in blood and urine of volunteers orally and dermally exposed to folpet were documented (Berthet *et al*., 2011a,b). The objective of the present study was to use these new data to develop a biomathematical model to describe and better understand the toxicokinetics of folpet and its ring metabolites in humans. No such model has been developed so far to describe the toxicokinetics of folpet in humans.

MATERIALS AND METHODS

Data used for folpet model development

Model development was based on available published metabolism data (Gordon *et al*., 2001) along with the human time-course data newly collected in volunteers (Berthet *et al*., 2011a,b). In this controlled experiment of Berthet *et al*. (2011a,b), healthy volunteers were exposed orally to 1 mg/kg of folpet or dermally to 10 mg/kg of folpet. The detailed time courses of PI in plasma and in urine were determined during a 96-h period post-dosing. Only urine time courses for PA_{eq} were documented during a 96-h period post-dosing.

Conceptual and functional representation of folpet model

The kinetics of PI and of PA_{eq} were modeled separately. Conceptual representations are depicted in Fig. 2 and Fig. 3. Symbols and abbreviations are defined in Table 1. The mathematical implementation of the models as systems of first-order differential equations is given in Table 2. In the modeling, it was considered that absorbed folpet is almost instantaneously broken down into its ring- and thiol-metabolites, leading respectively to PI and TTCA metabolites. However, only the pathway leading to the formation of the PI and PA_{eq} biomarkers of exposure was modeled in the current work.

The kinetics of folpet and its ring-metabolites (monitored PI and the sum of ring-metabolites, PA_{eq}) were modeled for different routes-of-exposure: oral, dermal and inhalation. The input doses per unit of time, bioavailable at each site of absorption, the skin, the respiratory tract and the GI tract, were thus respectively described as $g_{dermal}(t)$, $g_{inh}(t)$ and $g_{oral}(t)$. To simulate oral exposure, the model considers compartments for folpet in the GI ($G_{FT}(t)$) and for the almost instantaneously generated PI (G_{PI}) and ring-metabolites of PI (G_{PAA} and G_{PA}). Compartments were also used to represent the body burden of experimentally relevant PI, PAA and PA ring metabolites in blood and in tissues in dynamical equilibrium with blood, *i.e.* tissues that rapidly reach and maintain a fixed ratio with blood (referred to later as the blood compartment $B_{PI}(t)$, $B_{PAA}(t)$ and $B_{PA}(t)$, respectively, for simplicity). Other non-monitored ring-metabolites ($B_{ON}(t)$) were also represented as body compartments. Similarly, different excretion compartments were introduced to represent the amounts of PI, PAA and PA metabolites in urine and faeces, that is urinary compartments $U_{PI}(t)$, $U_{PAA}(t)$ and $U_{PA}(t)$, or faecal compartments $F_{PI}(t)$, $F_{PAA}(t)$ and $F_{PA}(t)$; other excretion compartments were added to describe the non-monitored ring-metabolites in urine ($U_{ON}(t)$) as well as in faeces ($F_{ON}(t)$).

To simulate the kinetics of PI specifically, PAA and PA compartments were grouped whereas to simulate the kinetics of PA_{eq}, PI, PAA and PA compartments were lumped. The compartments proposed for body metabolites and for excretion are based on the published data and appear sufficient in number to capture, for quantitative assessments, the essential

features of the kinetics of the measured metabolites. The linear elimination of PI from blood observed in Berthet *et al.* (2011a) suggests the absence of a significant storage of folpet in the body, either as an accumulation in lipids or a binding to tissue proteins, and indicates that the whole body distribution of folpet ring-metabolites can be described using a single compartment B(t) with first order elimination.

To simulate the kinetics of PI specifically in blood and urine following dermal absorption, the epidermis and the dermis were represented as separate compartments ($SE_{FT}(t)$ and $SD_{PI}(t)$, respectively). On the other hand, when simulating the kinetics of PA_{eq}, only the epidermal compartment was represented ($SE_{FT}(t)$) given the absence of measured blood time course of PA_{eq}, which simplifies model representation. Thus, all the specific features related to the modeling of dermal kinetics of PI specifically were shadowed by the important amounts of PAA and PA produced at the site-of-entry and contributing to total PA_{eq}.

On the contrary, simulations showed that it was not necessary to add a respiratory tract compartment as an input since the rapid absorption of folpet through the respiratory tract can be viewed kinetically as an almost constant intravenous exposure; thus, inhalation exposures were modeled by direct inputs to the blood compartment and instant fragmentation at the N-S link. This route-of-exposure was represented simply to show that it can be accounted for in the model. However, there is no available experimental data to date on the time course of ring biomarkers following inhalation exposure to folpet. To insure conservation of mass, all amounts were initially expressed on a mole basis to run the model.

Once the model was functionally represented by systems of differential equations (see Table 2), solving these equations yielded the mathematical functions for the time courses of folpet and each of its relevant metabolites in the different compartments. Initial conditions for every compartment were set to be zero at starting time of the kinetic modeling.

Determination of folpet model parameters

Model parameters were then determined by best-fit adjustments of the analytical solutions of differential equations to the data of Berthet *et al*. (2011a,b) on the time courses of PI in plasma and PI and PA_{eq} urine of volunteers orally and dermally exposed to folpet. MathCad 14 software was used for this purpose (PTC (Parametric Technology Corporation), Needham, MA, USA).

Several procedures exist to best-fit general analytical functions to data sets. For fitting, the algorithm genfit (included in Mathcad) was used, which essentially reproduces a least square minimization. To simplify differential equations and allow a first estimate of parameter values, use was made of the different time scales during which the various biological processes occur (e.g., time of absorption, distribution, metabolism, and excretion). Usually, in time, any exposure biomarker of interest finds its way to the final elimination site but on different time scales. The exact body location of a particular metabolite in time will depend

on the relative time scales of biological processes. Considering these time scales, in many cases, analytical solutions simplify to single exponential functions. For example, following a single oral exposure, the function describing blood time course of PI ($B_{PI}(t)$) will completely be driven by the overall rate of elimination of PI from blood (defined by k_B) and will be independent of the oral absorption dynamics (described by the overall disappearance rate of PI from the GI, k_G). In this case, $k_B << k_G$, such that the blood time course of PI ($B_{PI}(t)$) reduces to:

$$B_{PI}(t) \xrightarrow{k_B \ll k_G} \frac{k_{GB} D}{k_G} e^{-k_B t}. \quad (1)$$

Similarly, inhaled folpet is promptly absorbed into blood (in the order of min) such that the rate of appearance of PI in urine will only be limited by the overall elimination rate of PI from blood.

Moreover, when comparing oral and dermal rate time courses of PI, it was observed that elimination slopes were similar. The parallelism indicates that the final elimination phase of PI following dermal exposure is not governed by skin absorption rate (neither the rate of epidermal diffusion of folpet (k_{SESD}) or the diffusion rate of PI almost instantaneously formed in the dermis (k_{SDB})) but is rather driven by the overall elimination rate of PI from blood, k_B, as in the case of oral administration. The same holds true for PA_{eq}.

When looking at the data of Berthet *et al*. (2011a,b) on the elimination rate of PI in blood and urine as a function of time considering a given route of exposure (oral or dermal), it was also shown that elimination slopes were similar for blood and urine, as expected. Therefore, the transfer rate of PI from blood to urine, k_{BU}, can straightforwardly be computed directly from each of the observed blood and urinary time courses of Berthet *et al*. (2011a,b) as follows:

$$k_{BU} = \frac{U_{PI}(t)}{\int_0^t dt' B_{PI}(t')}. \quad (2)$$

In other words, for a given route of administration, experimental ratios of cumulative urinary excretion of PI to the area under the curve of blood PI is equal to a constant, defined as k_{BU} ($U_{PI}(t)$/AUC $B_{PI}(t) \sim k_{BU}$), and thus follow a quasi-constant trend in time. This is the behaviour required by our first-order model. Otherwise, the rates of elimination would not be a simple constant but would rather depend on the amounts of PI present in each compartment.

With regard to the oral route and overall disappearance rate of PI from the GI, represented by k_G, it is dependent not only on the absorption of PI from the GI tract into blood (k_{GB}), but also on the direct elimination of PI in faeces (without absorption) (k_{GF}) and GI metabolism of PI to other ring-metabolites (k_{GO}). The transfer rate k_{GB} of PI from the GI to blood can be

defined as a proportion f_b of the overall disappearance rate of PI from the GI (k_G). The transfer rates k_{GB}, k_{GO} and k_{GF} can in turn easily be defined as follows:

$$k_{GB} = f_b k_G, \quad (3)$$
$$k_{GF} + k_{GO} = (1 - f_b)k_G. \quad (4)$$

On the other hand, the dermal analogues to these parameters, the rate of epidermal diffusion of folpet (k_{SESD}), the diffusion rate of PI almost instantaneously formed in the dermis (k_{SDB}) and the dermal absorption fraction (f_{abs}), can be calculated in the same manner. For PA_{eq} parameters, a strategy similar to the one used to determine the parameters related to the kinetics of PI specifically can be used. With all the effective transfer rate parameters fixed, the model is completed and ready for sensitivity analysis.

Sensitivity analysis of folpet model parameters

There are several tests to measure the sensitivity of a particular parameter on a given function. Sensitivity analysis is the mathematical procedure aiming at assessing how much the value of a dependent function is modified as one changes a particular independent degree of freedom, while keeping all the remaining parameters unaffected. One can measure this effect by means of the normalized sensitivity coefficient defined as:

$$\sigma_s(\beta) = \frac{\beta}{\delta}\frac{f(\beta+\delta)-f(\beta)}{f(\beta)}. \quad (5)$$

This coefficient measures changes in model simulations defined by f with respect to the change δ of the parameter β under assessment. If the sensitivity coefficient is zero, the kinetic model is independent of the given parameter. If the coefficient diverges to infinity, simulation is highly sensitive to the model parameter and, therefore, the mathematical model is unstable. In our case, we have allowed all the degrees of freedom to vary a conservative standard deviation around the mean experimental data.

With this range of variability, the sensitivity coefficient for every degree of freedom in our model was calculated. This coefficient was computed for every single experimental time point and average values were then calculated.

Model evaluation

The model developed using the data of Berthet *et al*. (2011a,b) was evaluated using two independent sets of experimental data, namely plasma and urine time course data following both oral and dermal exposure. The kinetics of two different biomarkers was also modeled, namely PI specifically and PA_{eq}, hence allowing to verify the consistency between both mathematical simulations independently.

RESULTS

Development of folpet model and simulations of experimental kinetic data

Table 3 presents average parameter values of the model. Figure 4 shows that the model reproduces closely the data of Berthet *et al*. (2011a) on the average time courses of PI in blood and urine of volunteers exposed orally to folpet (R^2 of 0.663 and 0.989, respectively). With the same parameters, the model also simulated well the dermal data provided by Berthet *et al*. (2011b) on the average blood and urinary time courses of PI in volunteers (R^2 of 0.573 and 0. 976, respectively) (Fig. 5) as well as PA_{eq} values in urine (Fig. 6) (R^2=0.973 for oral and R^2=0.988 for dermal).

The good correspondence of our mathematical model with experimental data, using parameter values presented in Table 3, has corroborated our principal hypotheses about folpet kinetics, namely: a) it is almost instantaneous broken down to PI and its counterpart thiol metabolite at the site-of-entry (GI following oral exposure and dermis following dermal application); b) folpet ring-metabolites are rapidly absorbed into blood and then readily eliminated from the body following both oral and dermal exposures; c) the skin dermis does not retain folpet ring-metabolites, as the dermal absorption rate was found to be larger than the overall elimination rate of metabolites from blood; d) folpet is not stored in body compartments; e) PI is a specific biomarker of folpet exposure but is only a minor metabolite; f) the kinetics of PI is similar to that of total ring metabolites, expressed as PA_{eq}, but the latter is a much more abundant biomarker, although less specific to folpet.

Overall elimination half-life of PI from blood was found to be 39.9 h following oral exposure as compared to 34.3 h following dermal application. By comparison, the overall elimination half-life of PA_{eq} was found to be 28.0 h following oral administration as compared to 29.3 h after dermal application. These values indicate a fairly rapid tissue distribution, biotransformation and elimination of both PI and PA_{eq}, with values in the same range for both biomarkers (PI and PA_{eq}) and both routes-of-entry (oral and dermal). According to the model, four different processes contribute to total elimination rate of PI specifically from blood: biotransformation to other ring-metabolites, faecal excretion, renal clearance and finally distribution to non-observed organs. Of all the preceding mechanisms, renal clearance contributes mainly to the overall elimination rate of PI from blood (85.5%) following oral administration. On the other hand, following dermal application, renal clearance contributed only to 27.0% of PI overall elimination from blood, the remaining being attributed to metabolism of PI into derivatives or faecal excretion of blood PI.

When modeling the kinetics of total ring-metabolites, it was not possible to extract the exact contribution of the renal and faecal clearance to the overall elimination rate of PA_{eq} from the blood compartment, because only the time course of PA_{eq} in urine was experimentally

available (not blood). However, following oral exposure in volunteers, considering that the elimination of PA_{eq} in urine is almost complete 96 h post-exposure, it can roughly be estimated with the model that 24.5% of ingested folpet is eliminated as PA_{eq} in urine while the remaining 75.5% should either be eliminated as PA_{eq} in faeces or be found as unaccounted metabolites. Similarly, with the model, 7.42% of folpet were predicted to be absorbed through the skin, with 24.7% of absorbed amounts being excreted as PA_{eq} in urine and 75.3% as PA_{eq} in faeces or as unaccounted metabolites in the body.

From the time course curves of PI in blood, other calculated parameters include the discrete version of the area under the concentration-time curve (AUC), the area under the first moment of concentration–time curve (AUMC), the clearance from blood (CL), the apparent volume of distribution (V_d) and the mean residence time (MRT) as presented in Table 4. When looking at the predicted blood time course of PI (described by the analytical function $B_{PI}(t)$), maximum level for an oral exposure was obtained at around 4 h (and representing 0.0325% of ingested dose according to simulations as compared to 0.0397% of dose experimentally observed). This is simply due to competing rates of oral absorption and elimination of PI from the blood compartment. By comparison, following dermal application, this concomitant impact of absorption and elimination rates causes the blood profile to present a maximum level of PI at around 10 h. After dermal exposure, maximum level was lower than after ingestion (representing 0.00697% of applied dose according to simulations as compared to 0.0123% of dose experimentally observed), due to the small dermal absorption fraction, and time to maximum level is slightly delayed by the transfer rate through the skin.

Furthermore, it is interesting to note that the time course of PI in blood was parallel to that of PI urinary excretion rate, for both oral and dermal exposures, which indicates that the kinetics of PI is well described by considering solely the compartments $B_{PI}(t)$ and $U_{PI}(t)$. For example, in the oral model, if there were some crucial phenomenon occurring in the kidney, the blood and urinary time profiles would not necessarily evolve in parallel. Moreover, a single exponential elimination was apparent from slopes of the time course curves of PI in blood. This is an important indicator of the absence of any kind accumulation of PI in the body, which would then be reflected by at least a bi-exponential decrease rather than a mono-exponential elimination.

Regarding biotransformation of PI into its derivatives more specifically, it was taken to occur at the site-of-entry (GI or dermis following oral and dermal exposure, respectively) or as soon as PI reaches systemic blood. Given that PI is simulated to be largely metabolized to derivatives in the GI tract, the fraction of PI itself absorbed from the GI into blood is found to be very small (0.0353%). As for the importance of metabolism of PI to other ring-metabolites in blood, it could not be determined precisely for lack of faecal time course data. Therefore, only the concomitant contribution of metabolism of PI to derivatives and faecal excretion to the overall elimination of PI from the blood compartment could be computed, namely, 14.5% for oral exposure and 73.0% for dermal application (with the rest corresponding to renal clearance of PI).

In the particular case of model simulation of skin absorption and ensuing dermal kinetics of PI, separate skin sub-compartments had to be described. The first segment (SE_{FT} for folpet) is the one that effectively represents the dynamics of the absorption of folpet through the epidermis. By definition, the first segment describes the passive diffusion of unchanged folpet. The effective rate of diffusion of folpet was found to be $K_{SESD}= 2.22\times10^{-1}$ h^{-1}. The second segment (SD_{PI} for PI) simply represents the dermis which is irrigated by blood and therefore allows for the folpet to instantaneously biotransform into PI. Thus, this compartment accounts for the formation of PI and its rate of transfer from skin to blood with a half-life of 51.5 min. To model the toxicokinetics of PA_{eq} and not just PI specifically following dermal exposure, the toxicokinetic parameters describing skin absorption of folpet (absorption fraction and absorption rate) were taken to be the same as the ones calculated from the blood time course curves of PI; therefore, the dermal absorption fraction was set to be 0.0742 and the dermal absorption rate of folpet was taken to be $k_{SESD} =2.22\times10^{-1}$ h^{-1}. Interestingly, when comparing this value with the overall rate of appearance of PI in blood following oral exposure (k_G, otherwise defined as the rate of disappearance from the GI), which is calculated to be 1.06 h^{-1}, dermal absorption rate appears quite rapid.

Sensitivity analysis of model parameters

Sensitivity coefficients were computed for every single experimental time point and average values were calculated as reported in Table 5. The most sensitive parameters were those expected to shift the simulations by simple y-axis translation (the oral absorption fraction f_b, the dermal absorption fraction f_{abs} and the rate of elimination of PI or PA_{eq} from blood to urine k_{BU} and k''_{BU}), while the shape of the curves were mostly sensitive to changes in the slope defined by the overall elimination rate of PI or PA_{eq} from blood, k_B or k''_B, the overall disappearance rate of PI or PA_{eq} from the GI after oral exposure, k_G and k''_G, and the dermal absorption rate k_{SESD}. With respect to k_{SDB}, the analysis also showed an important effect of its variation on the time course curves. Due to the fact that folpet is rapidly absorbed, any variation in the transfer rates from the epidermis to dermis and/or variation in the metabolism at the site-of-entry will result in a phenomenon similar to a time delay or a translation on the time-axis.

DISCUSSION

This study allowed a better understanding of the kinetics of PI, PA_{eq} as potential key biomarkers of exposure to folpet. It enabled to relate an internal dose of folpet to the time courses of PI and PA_{eq} biomarkers in available biological fluids (such as blood and urine). Effective compartment models, with two mathematical components, were built to represent the kinetics of those biomarkers. The toxicokinetic models provided a very good approximation of the experimental time course data of Berthet *et al*. (2011a,b) in volunteers orally and dermally exposed to folpet under controlled conditions.

According to model simulations and in line with Gordon (2010), the first biological process governing the kinetics of folpet is its almost instantaneous non-enzymatic breakdown into PI and thiophosgene. PI biotransformation into PA and PAA at the sites-of-entry (GI for oral exposure and dermis for dermal exposure) was also found to be relatively rapid. Once in blood, PI elimination was found to be fairly rapid (k_B=31.6 h) and was modeled to occur through metabolism to PAA and PA, renal clearance and fecal excretion. On the other hand, when simulating the time course of PA_{eq}, which accounts for total ring-metabolites, elimination from blood was dependent only on renal and biliary clearance. Levels of PI and PA_{eq} in non monitored tissues (such as liver, kidney or lung) were taken to rapidly reach a dynamical equilibrium with blood and were theoretically assumed to evolve in parallel. PI and PA_{eq} in blood and these tissues were thus lumped under a single compartment defined as PI or PA_{eq} blood compartment for simplicity.

The excellent agreement between model simulations and measured blood and urinary time course data following an oral and dermal exposure in volunteers, considering a single-exponential model for PI and PA_{eq} elimination from blood and tissues in dynamical equilibrium with blood, also confirmed the lack of significant storage of the parent compound or the metabolites in any tissue components (e.g. adipose tissues, protein binding as well as other body lipid components). This is in line with animal studies showing negligible accumulation of phthalimide moieties (Couch *et al*., 1977; Ackermann *et al*., 1978) in tissues following oral or intraperitoneal administration of labelled folpet.

In the particular case of model simulation of an oral exposure in humans, a single GI compartment was introduced to describe site-of-entry kinetics of PI and PA_{eq} and account for GI metabolism, absorption in blood as well as the intestinal transit time which delays appearance of PI and PA_{eq} in faeces (in the latter case with a half-life of 39.1 min for PI specifically and of 31 min for PA_{eq}). Following folpet ingestion in humans, even though it is almost instantaneously broken down into PI in the GI, only a very small fraction of PI reaches blood (0.0353% according to the model). This result can be *a priori* be understood as an efficient elimination of folpet and/or PI directly through faeces without being absorbed. However, experimental data in rats show that following oral or intraperitonal administration of ring-labelled folpet, between 90 and 100% of the administered dose were excreted in the

urine of rats over a 24-h period post-dosing (Wood *et al*., 1991; Couch *et al*., 1977). Therefore, the small amounts of PI transferred to blood following ingestion of folpet can only be explained by a rapid biotransformation of PI into PAA and PA in the GI, the latter of which are subsequently readily absorbed into systemic blood.

It is also noteworthy that the mathematical model did not require consideration of an enterohepatic recycling of any ring metabolite, as no feedback features were apparent from the available blood time course data in volunteers (Berthet *et al*., 2011a,b). Therefore, contribution of this process to the overall excretion dynamics was found negligible and thus had no impact on the kinetics of distribution and elimination of these metabolites.

On the other hand, to simulate dermal exposure, PI in the skin was represented by two sub-compartments. As previously mentioned, the first segment simply represents passive diffusion of folpet through the epidermis (3.13 h) while the second accounts for the actual formation, metabolism and dynamics of PI in the dermis with a half-life of 51.5 min. The latter time scales show the rapid skin absorption when exposed to folpet in humans. While folpet dermally absorbed is quickly metabolized at the site-of-entry and readily distributed to the systemic blood compartment, only a small fraction of applied folpet penetrates the skin barrier (7.42% according to the model). This is in agreement with the rat data from the only dermal penetration study on folpet in animals, showing a low dermal absorption fraction (Shah *et al*., 1987). With respect to model simulation of PA_{eq} kinetics following dermal exposure, the toxicokinetic parameters describing skin absorption of folpet (absorption fraction and absorption rate) were taken to be the same as the ones calculated from the blood time course curves of PI.

Once applied folpet reaches the dermis, which is irrigated by blood, it was modeled to be almost instantaneously metabolized to PI. This is supported by the available *in vitro* data of Gordon *et al*. (2001) showing that the half life of ^{14}C-labelled folpet (1 mg/L) added to human blood was estimated to be in the order of second (4.9 s). In the model, PI is in turn mostly metabolized to PAA and PA at the site-of-entry. The PI reaching the blood compartment is predicted to be eliminated in large part by renal clearance (representing 88.5% of overall elimination according to the model) while the rest (11.5%) represents PI metabolism and fecal excretion. Most plausibly, faecal excretion is very limited according to animal data (Couch *et al*., 1977). Unfortunately, even if our toxicokinetic model accounted for these processes, the experimental data available in humans did not include faecal matrix.

With respect to renal clearance more specifically, the parallelism observed between the blood and the urine compartments is clear evidence that the kidney is in complete kinetic equilibrium with blood and that no particular retention mechanism occurs for PI in the kidney. Furthermore, according to model simulations, no saturation in absorption, distribution, metabolism of PI or urinary excretion was apparent at the 1 mg/kg oral and 10 mg/kg dermal doses administered to subjects.

CONCLUSION

This study succeeded in developing a toxicokinetic model for PI and the sum of ring metabolites PI, PAA and PA, which provided a close match to a large set of experimental time course data in two biological matrices of exposed volunteers. This modeling provided new insights into the mechanistic determinants of folpet kinetics that can serve for a better understanding and use of ring-metabolites as proper biomarkers.

ACKNOWLEDGEMENTS

This study was funded by the ANSES (Agence Nationale de Sécurité Sanitaire de l'alimentation, de l'environnement et du Travail). The authors would like to acknowledge the Swiss team for this nice collaboration.

REFERENCES

Ackermann H, Faust H, Kagan YS, Voronina VH. 1978. Metabolic and Toxic Behaviors of Phthalimide Derivatives in Albino-Rat .2. Placental Passage of Chloromethyl Phthalimide, Oxymethyl Phthalimide, and Phthalimide - Their Fetal Metabolism. *Arch. Toxicol.* **40**: 255-261.

Berthet A, Bouchard M, Danuser B. 2011a. Toxicokinetics of captan and folpet biomarkers in orally exposed volunteers. *J. Appl. Toxicol.* (in press). DOI 795151-668048.

Berthet A, Bouchard M, Vernez D. 2011b. Toxicokinetics of captan and folpet biomarkers in dermally exposed volunteers. *J. Appl. Toxicol.* (in press). DOI 10.1002/jat.1659.

Blount BC, Milgram KE, Silva MJ, Malek NA, Reidy JA, Needham LL, Brock JW. 2000. Quantitative detection of eight phthalate metabolites in human urine using HPLC-APCI-MS/MS. *Anal. Chem.* **72**: 4127-4134.

Canal-Raffin M, Receveur M, Martinez B, Titier K, Ohayon C, Baldi I, Molimard M, Moore N, Brochard P. 2008. Quantification methods of folpet degradation products in plasma with HPLC-UV/DAD: Application to an in vivo toxicokinetic study in rats. *J. Chromatogr. B-Anal. Technol. Biomed. Life Sci.* **865**: 106-113.

Chasseaud L, Hawkins DR, Franklin ER, Weston KT. 1974. The metabolic fate of 14C-Folpet (Phaltan) in the rat (Folpet). Huntingdon Research Centre Ltd.: Huntingdon. Unpublished report No CHR1-74482.

Chasseaud L. 1980. (Carbonyl-14C) Folpet metabolism in rats. Huntingdon Research Centre Ltd.: Huntingdon. Unpublished report No DPBP 51202.

Couch RC, Siegel MR, Dorough HW. 1977. Fate of captan and folpet in rats and their effects on isolated liver nuclei. *Pestic. Biochem. Physiol.* **7**: 547-558.

Gordon EB. 2010. Captan and folpet. In Handbook of pesticide toxicology, Krieger R, (ed), Elsevier: New York; 1915-1949.

Gordon EB, Ehrlich T, Mobley S, Williams M. 2001. Measurement of the reaction between the fungicides captan or folpet and blood thiols. *Toxicol. Meth.* **11**: 209-223.

Guo YLL, Wang BJ, Lee CC, Wang JD. 1996. Prevalence of dermatoses and skin sensitisation associated with use of pesticides in fruit farmers of southern Taiwan. Occup. *Environ. Med.* **53**: 427–431.

Lebailly P, Devaux A, Pottier D, De Meo M, Andre V, Baldi I, Severin F, Bernaud J, Durand B, Henry-Amar M, Gauduchon P. 2003. Urine mutagenicity and lymphocyte DNA damage in fruit growers occupationally exposed to the fungicide captan. *Occup. Environ. Med.* **60**: 910-917.

Lisi P, Caraffini S, Assalve D. 1987. Irritation and sensitization potential of pesticides. *Contact Dermat.* **17**: 212–218.

Shah PV, Fisher HL, Sumler MR, Monroe RJ, Chernoff N. 1987. Comparison of the Penetration of 14 Pesticides Through the Skin of Young and Adult-Rats. *J. Toxicol. Environ. Health* **21**: 353-366.

Silva MJ, Samandar E, Preau JL Jr., Reidy JA, Needham LL, Calafat AM. 2007. Quantification of 22 phthalate metabolites in human urine. *J. Chromatogr. B Analyt. Technol. Biomed. Life Sci.* **860**: 106-112.

United States Environmental Protection Agency (USEPA). 1990. Registration eligibility decision (RED) – Folpet. Washington D.C., US Environmental Protection Agency. 212

United States Environmental Protection Agency. 1975. Initial Scientific and Mini-economic Review of Captan. Report no. EPA/540-1-75-012. Office of Pesticide Programs, Criteria and Evaluation Division: Washington.

Williams DT, Blanchfield BJ. 1974. Retention, excretion and metabolism of phthalic acid administrated orally to the rat. *Bull. Environ. Contam. Toxicol.* **12**: 109-112

Wood SG, Chasseaud LF, Cheng K, Hall M, Fitzpatrick K, Iqbal S, Barlett A. 1991. Metabolic fate of 14C-folpet in Sprague-Dawley rats. Unpublished report No HRC/MBS 41/91499 from Huntingdon Life Sciences Limited, Woolley Road, Alconbury, Huntingdon, Cambridgeshire. Submitted to WHO by Makhteshim Chemical Works, Beer-Sheva, Israel.

Zainal H, Que Hee SS. 2003. Folpet permeation through nitrile gloves. *Appl. Occup. Environ. Hyg.* **18**: 658-668.

Table 1. Symbols used in the functional representation of the model

Model parameter	Units	Description
$G_{FT}(t)$	mol	Amounts of folpet in the GI as a function of time
$G_{PI}(t)$	mol	Amounts of PI in the GI as a function of time
$G_{PAA}(t)$	mol	Amounts of PAA in the GI as a function of time
$G_{PA}(t)$	mol	Amounts of PA in the GI as a function of time
$SE_{FT}(t)$	mol	Amounts of folpet in the epidermis as a function of time
$SD_{PI}(t)$	mol	Amounts of PI in the dermis as a function of time
$SD_{PAA}(t)$	mol	Amounts of PAA in the dermis as a function of time
$SD_{PA}(t)$	mol	Amounts of PA in the dermis as a function of time
$B_{PI}(t)$	mol	Burden of PI in the blood compartment as a function of time
$B_{PAA}(t)$	mol	Burden of PAA in the blood compartment as a function of time
$B_{PA}(t)$	mol	Burden of PA in the blood compartment as a function of time
$B_{ON}(t)$	mol	Burden of non-monitored ring-metabolites in the blood compartment as a function of time
$F_{PI}(t)$	mol	Amounts of PI excreted in faeces as a function of time
$F_{PAA}(t)$	mol	Amounts of PAA excreted in faeces as a function of time
$F_{PA}(t)$	mol	Amounts of PA excreted in faeces as a function of time
$F_{ON}(t)$	mol	Amounts of non-monitored ring-metabolites in faeces as a function of time
$U_{PI}(t)$	mol	Amounts of PI excreted in urine as a function of time
$U_{PAA}(t)$	mol	Amounts of PAA excreted in urine as a function of time
$U_{PA}(t)$	mol	Amounts of PA excreted in urine as a function of time
$U_{ON}(t)$	mol	Amounts of non-monitored ring-metabolites excreted in urine as a function of time
k_{GB}	h^{-1}	Rate of PI absorption from the GI into the blood compartment
k_{GF}	h^{-1}	Rate of faecal elimination of unabsorbed PI (directly from the GI)
k_{GO}	h^{-1}	Rate of PI biotransformation to other non-monitored ring-metabolites in the GI
k_G	h^{-1}	Rate of overall disappearance of PI from the GI either through absorption in blood, metabolism to other ring-metabolites or excretion in faeces ($k_{GB}+k_{GO}+ k_{GF}$)
k''_{GB}	h^{-1}	Rate of total ring-metabolites (sum of PI, PAA and PA expressed as PA_{eq}) absorption from the GI into the blood compartment
k''_{GF}	h^{-1}	Rate of faecal elimination of unabsorbed total ring-metabolites (sum of PI, PAA and PA expressed as PA_{eq}) (directly from the GI)
k''_{G}	h^{-1}	Rate of overall disappearance of total ring-metabolites (sum of PI, PAA and PA expressed as PA_{eq}) from the GI either through absorption in blood. or excretion in faeces ($k''_{GB}+ k''_{GF}$)
k_{BB}	h^{-1}	Rate of PI biotransformation to other non-monitored ring-metabolites in the body
k_{BU}	h^{-1}	Transfer rate of PI from blood to urine
k_{BF}	h^{-1}	Transfer rate of PI from blood to faeces
k_B	h^{-1}	Overall elimination rate of PI from the blood compartment ($k_{BU}+k_{BF}+ k_{BB}$)
k''_{BU}	h^{-1}	Transfer rate of total ring-metabolites (sum of PI, PAA and PA expressed as PA_{eq}) from blood to urine

Model parameter	Units	Description
k''_{BF}	h^{-1}	Transfer rate of total ring-metabolites (sum of PI, PAA and PA expressed as PA_{eq}) from blood to faeces
k''_{B}	h^{-1}	Overall elimination rate of total ring-metabolites (sum of PI, PAA and PA expressed as PA_{eq}) from the blood compartment ($k''_{BU}+k''_{BF}$)
k_{SESD}	h^{-1}	Rate of epidermal diffusion of folpet
k_{SDB}	h^{-1}	Rate of diffusion of ring-metabolites in the dermis where they are almost instantaneously formed
k_{SDO}	h^{-1}	Rate of PI biotransformation to other non-monitored ring-metabolites in the dermis
f_{abs}		Dermal absorption fraction of folpet
f_b		Proportion of PI in the GI, which is transferred to blood
f_u		Proportion of blood PI excreted in urine
D(t)	mg/kg	Absorbed dose as a function of time

Table 2. First-order linear differential equations describing the kinetics of folpet and its PI, and PA_{eq} metabolites in each of the model compartments

Exposure route	Compartment	Differential equations	
		PI kinetics	PA_{eq}=PI+PAA+PA kinetics[a]
Oral	Gastrointestinal tract	$\frac{dG_{PI}(t)}{dt} = D\delta(t) - k_G G_{PI}(t)$	$\frac{dG_{PAeq}(t)}{dt} = D\delta(t) - k''_G G_{PAeq}(t)$
	Blood compartment	$\frac{dB_{PI}(t)}{dt} = k_{GB} G_{PI}(t) - k_B B_{PI}(t)$	$\frac{dB_{PAeq}(t)}{dt} = k''_{GB} G_{PAeq}(t) - k''_B B_{PAeq}(t)$
	Urine	$\frac{dU_{PI}(t)}{dt} = k_{BU} B_{PI}(t)$	$\frac{dU_{PAeq}(t)}{dt} = k''_{BU} B_{PAeq}(t)$
	Faeces	$\frac{dF_{PI}(t)}{dt} = k_{BF} B_{PI}(t) + k_{GF} G_{PI}(t)$	$\frac{dF_{PAeq}(t)}{dt} = k''_{BF} B_{PAeq}(t) + k''_{GF} G_{PAeq}(t)$
Dermal	Epidermis	$\frac{dSE_{FT}(t)}{dt} = f_{abs} D\delta(t) - k_{SESD} SE_{TI}(t)$	$\frac{dS_{PAeq}(t)}{dt} = f_{abs} D\delta(t) - k_{SESD} S_{PAeq}(t)$
	Dermis	$\frac{dSD_{PI}(t)}{dt} = k_{SESD} SE_{FT}(t) - k_{SDB} SD_{PI}(t)$	
	Blood compartment	$\frac{dB_{PI}(t)}{dt} = k_{SDB} SD_{PI}(t) - k_B B_{PI}(t)$	$\frac{dB_{PAeq}(t)}{dt} = k_{SESD} S_{PAeq}(t) - k''_B B_{PAeq}(t)$
	Urine	$\frac{dU_{PI}(t)}{dt} = k_{BU} B_{PI}(t)$	$\frac{dU_{PAeq}(t)}{dt} = k''_{BU} B_{PAeq}(t)$
	Faeces	$\frac{dF_{PI}(t)}{dt} = k_{BF} B_{PI}(t)$	$\frac{dF_{PAeq}(t)}{dt} = k''_{BF} B_{PAeq}(t)$

[a] The total amounts of ring metabolites, expressed as PA_{eq} are defined as follows: $G_{PAeq}(t) = G_{PI}(t) + G_{PAA}(t) + G_{PA}(t)$, $B_{PAeq}(t) = B_{PI}(t) + B_{PAA}(t) + B_{PA}(t)$, $S_{PAeq}(t) = S_{PI}(t) + S_{PAA}(t) + S_{PA}(t)$, $U_{PAeq}(t) = U_{PI}(t) + U_{PAA}(t) + U_{PA}(t)$ and $F_{PAeq}(t) = F_{PI}(t) + F_{PAA}(t) + F_{PA}(t)$.

Table 3. Model parameter values determined from the average blood and urinary time course data of Berthet *et al*. (2011a,b) in volunteers orally and dermally exposed to folpet

	Model parameters[a]		Values
PI kinetics	Transfer rates (h^{-1})	k_B	2.19×10^{-2}
		k_{BU}	1.24×10^{-2}
		k_G	1.06
		k_{GB}	3.75×10^{-4}
		$k_{GF}+ k_{GO}$	1.06
		k_{SESD}	2.22×10^{-1}
		$k_{SDB}+ k_{SDO}$	8.08×10^{-1}
		k_{SDB}	1.01×10^{-3}
		k_{SDO}	8.07×10^{-1}
	Fractional partition (%)	f_b	3.53×10^{-2}
		f_u	85.5
		f_{abs}	7.42
PA_{eq} kinetics [a]	Transfer rates (h^{-1})	k''_B	2.42×10^{-2}
		k''_{BU}	2.39×10^{-2}
		k''_G	1.39
		k''_{GB}	1.37
		k''_{GF}	1.39×10^{-2}
		k_{SESD}	2.22×10^{-1}
	Fractional partition (%)	f''_b	99.0
		f_u''	99.0
		f_{abs}	7.42

[a] Symbols and abbreviations used in this study are defined in Table 1.

Table 4. Toxicokinetic parameters derived from the average data of Berthet *et al.* (2011a,b) on the blood profile of PI following oral administration of 1 mg/kg of folpet or dermal application of 10 mg/kg

	First-order toxicokinetic values for PI	
	Oral	Dermal
Model parameters [a]		
AUC [b] [µmol hr/L]	0.918	1.69
AUMC [c] [µmol hr^2/L]	26.9	35.4
CL [d] [L/hr]	0.0944	0.133
Vd [e] [L]	4.30	6.05
MRT [f] [hr]	29.4	22.9

[a] Toxicokinetic parameters were calculated from the mean percentage of the dose profile.

[b] The discrete version of the area under the curve is calculated as: $\mathrm{AUC} = \frac{1}{2}\sum_{\forall i}(t_i\text{-}t_{i+1})\,[C(t_i) + C(t_{i+1})]$.

[c] The first moment of concentration-time curve is approximated by: $\mathrm{AUMC} = \frac{1}{2}\sum_{\forall i}(t_i\text{-}t_{i+1})\,[t_i C(t_i) + t_{i+1} C(t_{i+1})]$.

[d] The clearance of the blood module was determined by: $\mathrm{CL} = \frac{\mathrm{Dose}}{\mathrm{AUC}}$.

[e] The volume of distribution computed by: $V_d = \frac{\mathrm{CL}}{\beta}$.

[f] The mean residence time is defined as: $\mathrm{MRT} = \frac{\mathrm{AUMC}}{\mathrm{AUC}}$.

Table 5. Sensitivity coefficients of model parameters with variability range

Model parameters	Urinary average sensitivity coefficient		Blood average sensitivity coefficient	
	+δ	-δ	+δ	-δ
k_B (oral)	-0.255	0.311	-0.355	0.472
k_B (dermal)	-0.234	0.284	-0.301	0.397
f_b, f_{abs} and k_{BU} (oral and dermal)	1.00	-1.00	1.00	-1.00
k_G (oral)	0.0596	-0.0954	0.0162	-0.0381
k_{SESD} (dermal)	0.233	-0.343	0.239	-0.335
k_{SDB} (dermal)	0.909	-0.909	0.888	-0.888

Captions to Figures

Figure 1. Metabolic pathway of folpet according to available *in vivo* experiments in animals and *in vitro* studies.

Figure 2. Model conceptual representation of the kinetics of folpet with focus on PI and its ring-metabolites. Symbols and abbreviations are described in Table 1.

Figure 3. Model conceptual representation of the kinetics of folpet and its PA_{eq} ring-metabolites. Symbols and abbreviations are described in Table 1.

Figure 4. Model simulations (solid line) compared with experimental data of Berthet *et al.* (2011a) on A) the time course of PI in blood (% of dose) and B) the cumulative urinary excretion time courses of PI (% of dose) in five volunteers following an oral administration of 1 mg/kg bw of folpet (solid circles). Symbols represent average experimental values and vertical bars the experimental standard deviation (n = 5).

Figure 5. Model simulations (solid line) compared with experimental data of Berthet *et al.* (2011b) on A) the time course of PI in blood (% of dose) and B) the cumulative urinary excretion time courses of PI (% of dose) in five volunteers following a dermal application of 10 mg/kg bw of folpet (solid circles). Symbols represent average experimental values and vertical bars the experimental standard deviation (n = 5).

Figure 6. Model simulations (solid line) compared with experimental data of Berthet *et al.* (2011b) on the cumulative urinary excretion time course of PA_{eq} (% of dose) in five volunteers following A) an oral ingestion of 1 mg/kg bw of folpet and B) a dermal application of 10 mg/kg bw of folpet (solid circles). Symbols represent average experimental values and vertical bars the experimental standard deviation (n = 5).

Figure 1

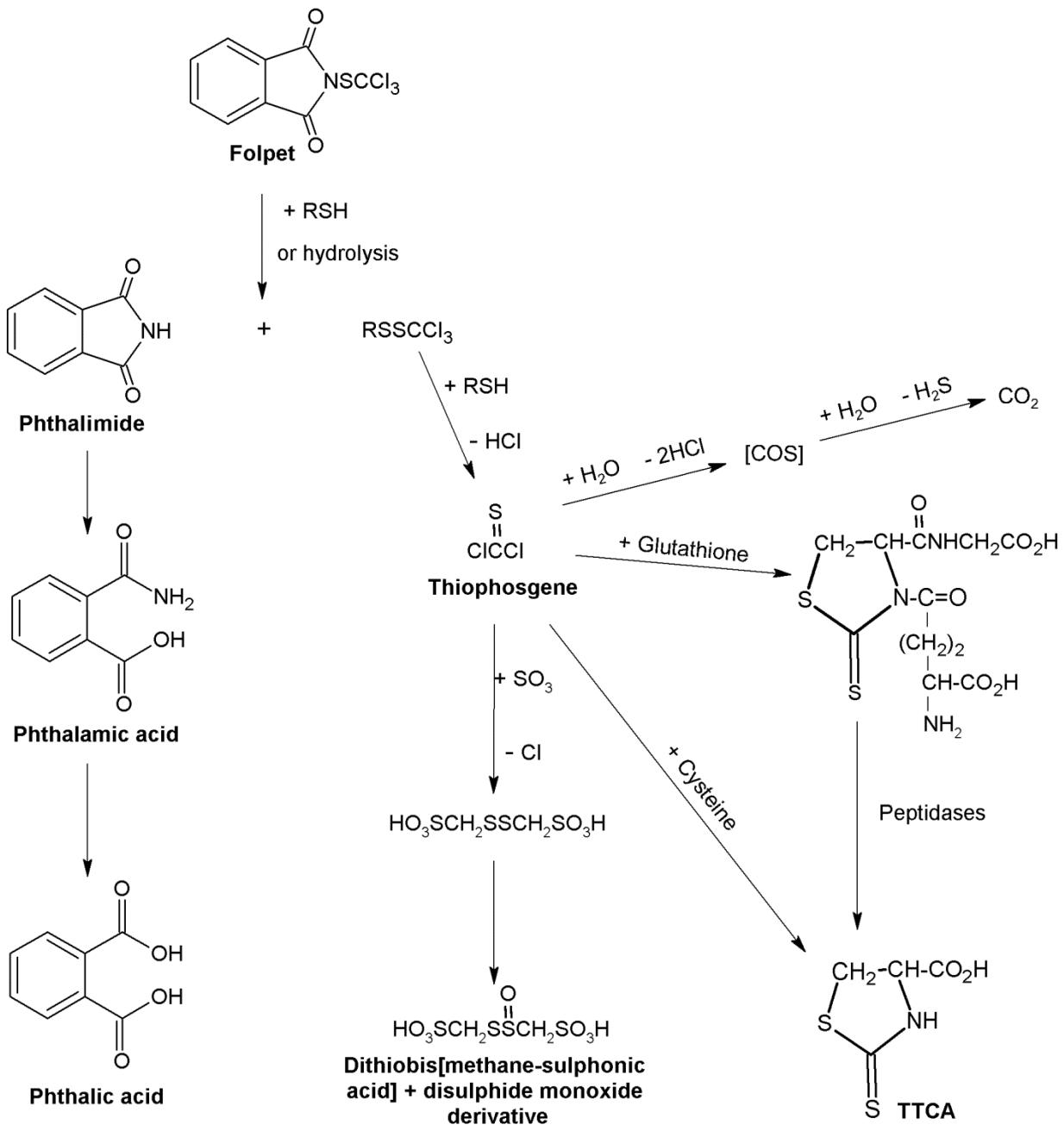
Folpet
+ RSH
or hydrolysis
Phthalimide
+
RSSCCl3
+ RSH
- HCl
+ H2O
- 2HCl
[COS]
+ H2O
- H2S
CO2
Thiophosgene
+ Glutathione
+ SO3
- Cl
HO3SCH2SSCH2SO3H
HO3SCH2SSCH2SO3H
Dithiobis[methane-sulphonic acid] + disulphide monoxide derivative
+ Cysteine
Peptidases
Phthalamic acid
Phthalic acid
TTCA

Figure 2

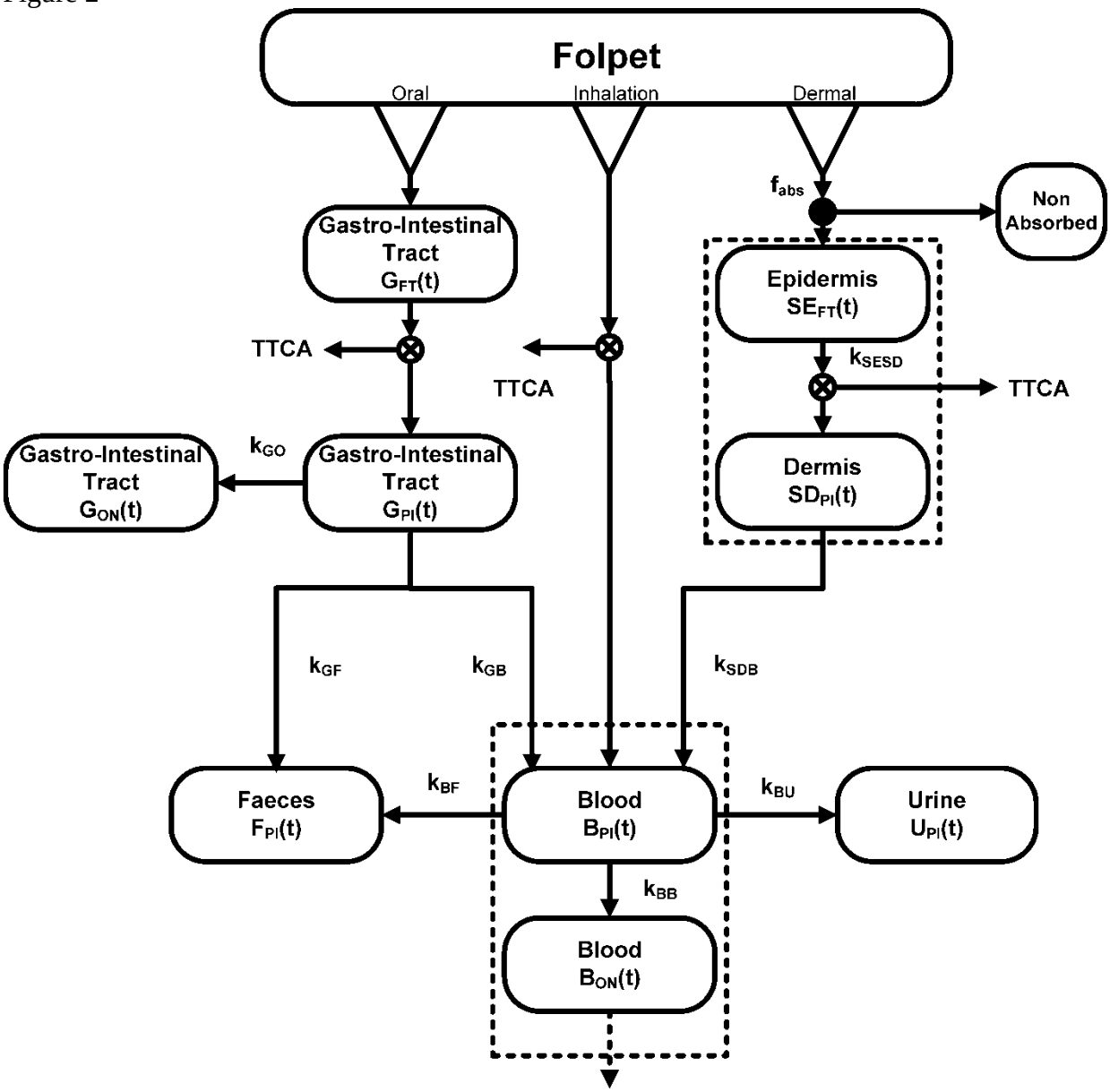
Folpet
Oral
Inhalation
Dermal
f_{abs}
Non Absorbed
Gastro-Intestinal Tract $G_{FT}(t)$
Epidermis $SE_{FT}(t)$
TTCA
TTCA
k_{SESD}
TTCA
Gastro-Intestinal Tract $G_{ON}(t)$
k_{GO}
Gastro-Intestinal Tract $G_{PI}(t)$
Dermis $SD_{PI}(t)$
k_{GF}
k_{GB}
k_{SDB}
Faeces $F_{PI}(t)$
k_{BF}
Blood $B_{PI}(t)$
k_{BU}
Urine $U_{PI}(t)$
k_{BB}
Blood $B_{ON}(t)$

Figure 3

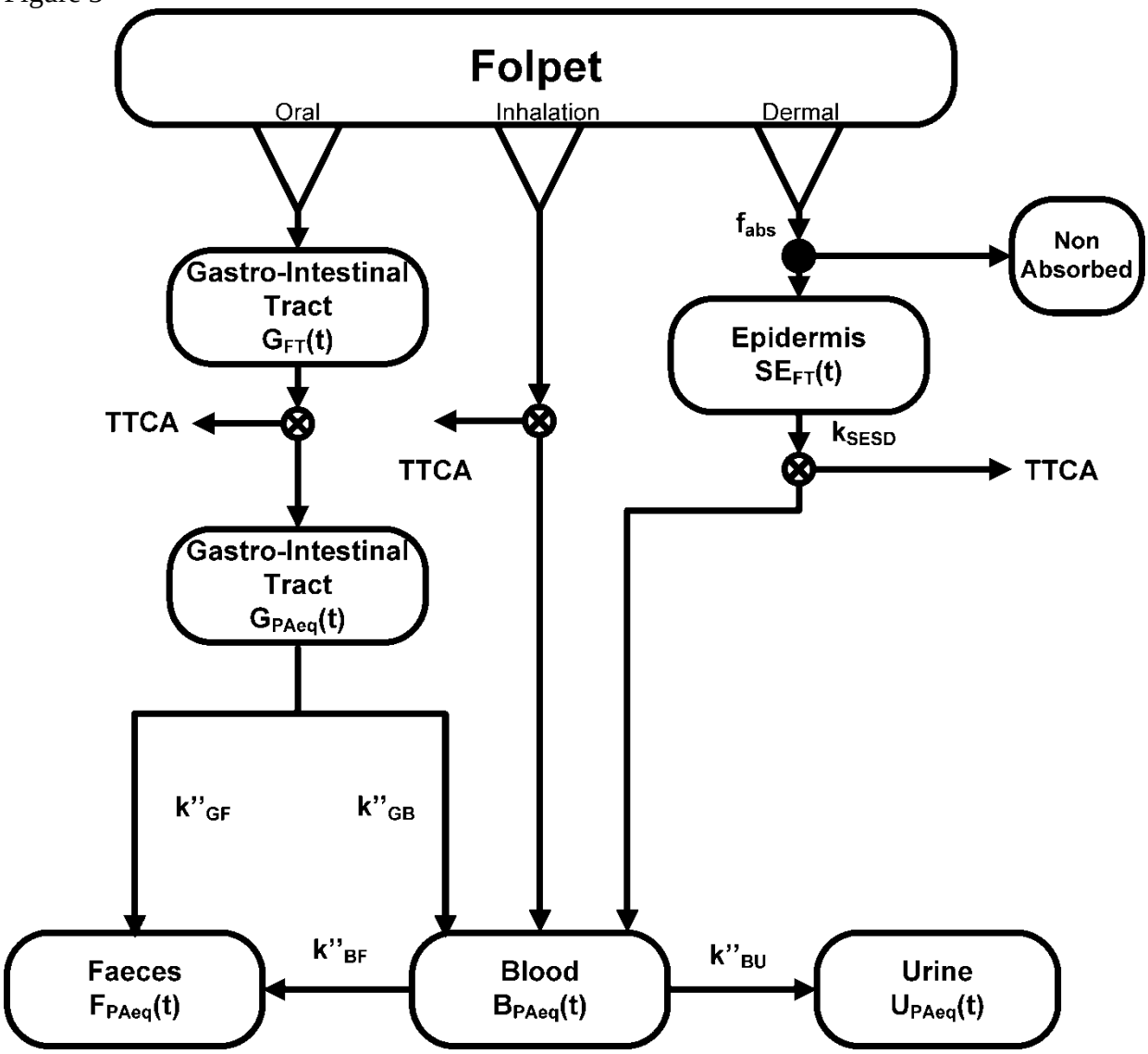
Folpet
Oral
Inhalation
Dermal
f_{abs}
Non Absorbed
Gastro-Intestinal Tract $G_{FT}(t)$
Epidermis $SE_{FT}(t)$
TTCA
TTCA
k_{SESD}
TTCA
Gastro-Intestinal Tract $G_{PAeq}(t)$
k''_{GF}
k''_{GB}
Faeces $F_{PAeq}(t)$
k''_{BF}
Blood $B_{PAeq}(t)$
k''_{BU}
Urine $U_{PAeq}(t)$

Figure 4

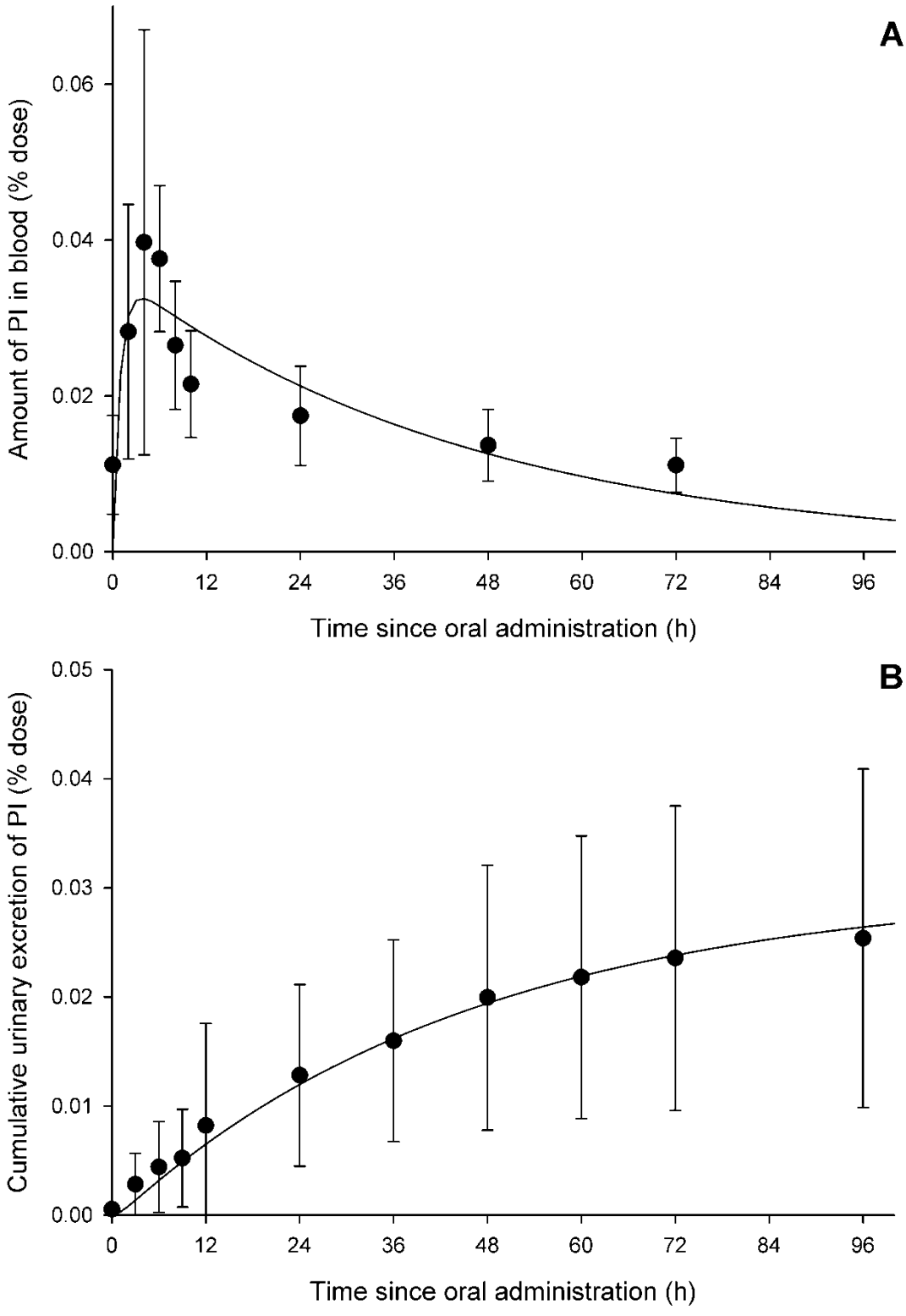
A
Amount of PI in blood (% dose)
0.00
0.02
0.04
0.06
0 12 24 36 48 60 72 84 96
Time since oral administration (h)
B
Cumulative urinary excretion of PI (% dose)
0.00
0.01
0.02
0.03
0.04
0.05
0 12 24 36 48 60 72 84 96
Time since oral administration (h)

Figure 5

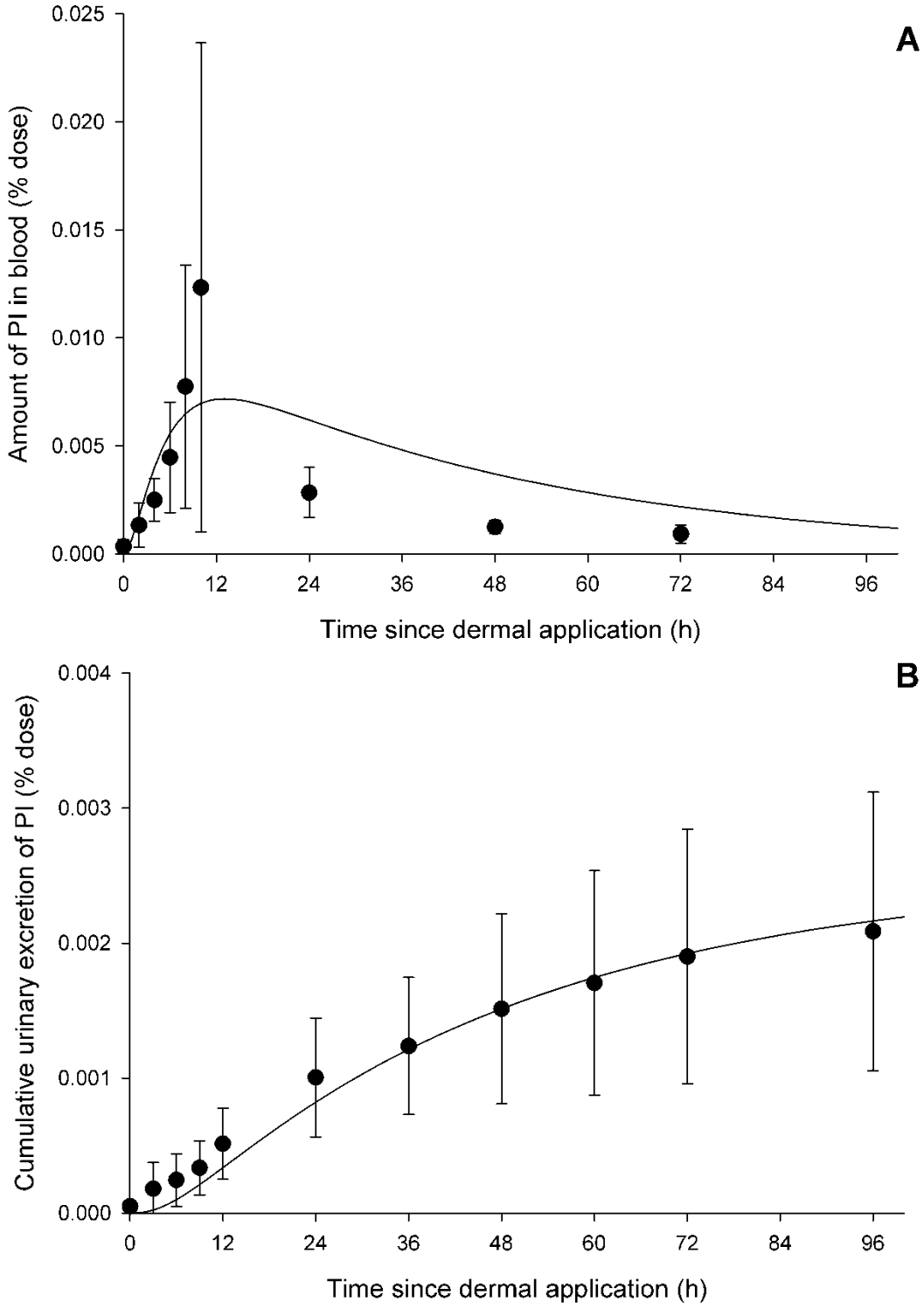
A
Amount of PI in blood (% dose)
0.025
0.020
0.015
0.010
0.005
0.000
0
12
24
36
48
60
72
84
96
Time since dermal application (h)
B
Cumulative urinary excretion of PI (% dose)
0.004
0.003
0.002
0.001
0.000
0
12
24
36
48
60
72
84
96
Time since dermal application (h)

Figure 6

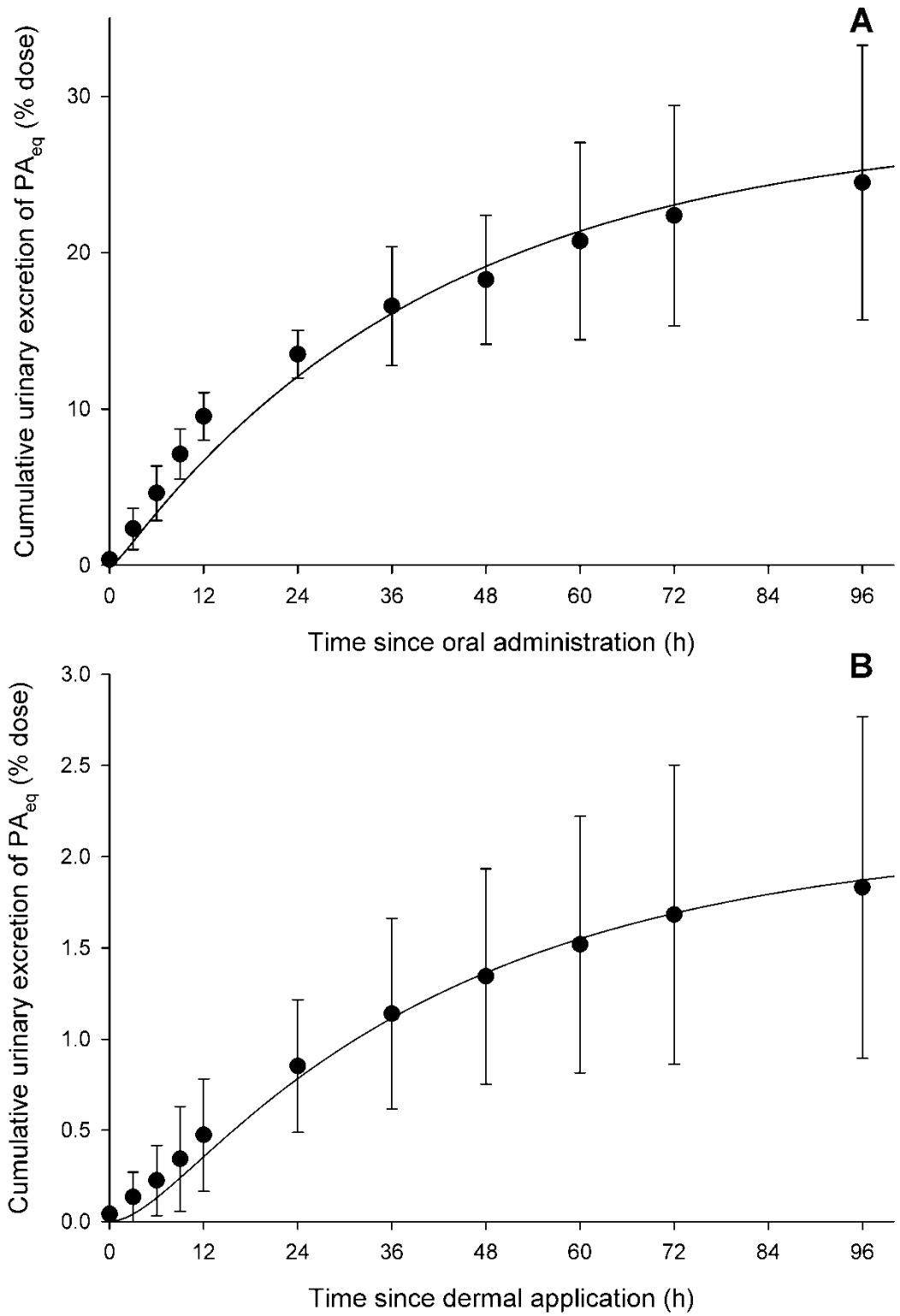
A
Cumulative urinary excretion of PAeq (% dose)
0
10
20
30
0
12
24
36
48
60
72
84
96
Time since oral administration (h)
B
Cumulative urinary excretion of PAeq (% dose)
0.0
0.5
1.0
1.5
2.0
2.5
3.0
0
12
24
36
48
60
72
84
96
Time since dermal application (h)